iScience, Volume *23*

Supplemental Information

In Vivo Bioengineering of Fluorescent Conductive Protein-Dye Microfibers

Maria Moros, Francesca Di Maria, Principia Dardano, Giuseppina Tommasini, Hiram Castillo-Michel, Alessandro Kovtun, Mattia Zangoli, Martina Blasio, Luca De Stefano, Angela Tino, Giovanna Barbarella, and Claudia Tortiglione

Supplemental information

Synthesis and characterization of DTTO and other thiophene based fluorophores

For DTTO (Scheme 1) the synthetic details, NMR and optical characterizations have been previously reported.(Palama et al., 2011) The control fluorophores ECB04, compound 2 and compound 3, have also been previously characterized (Palama et al., 2011).

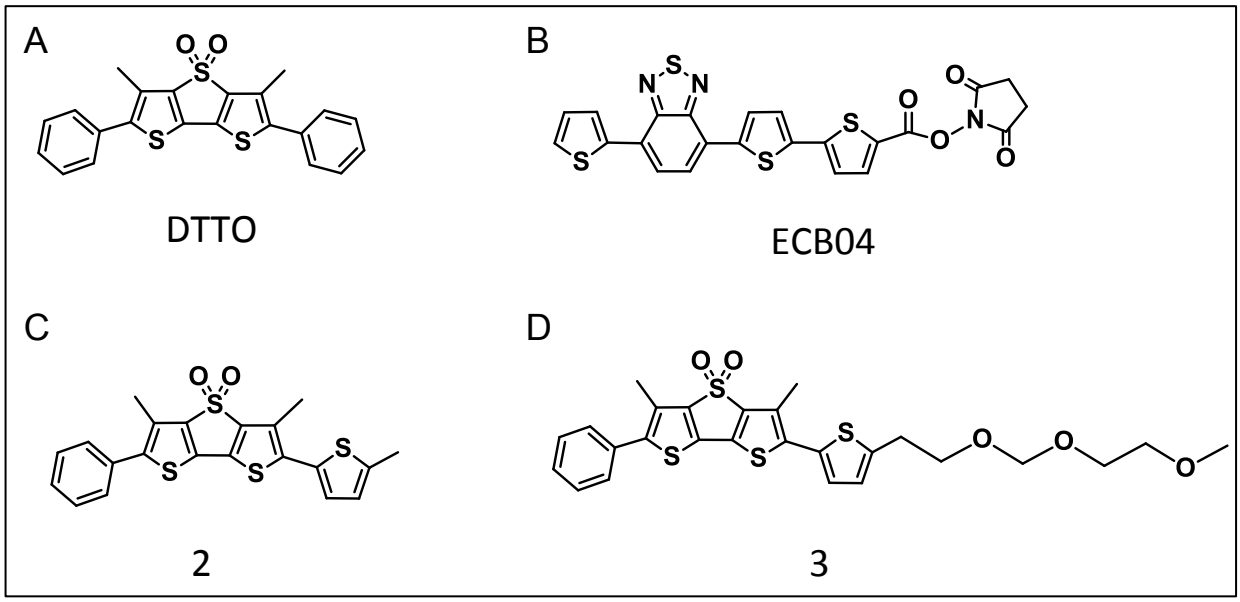

Scheme S1. Molecular structure of thiophene based fluorophores. Related to Figure 1, Figure S1, Figure S4, and Figure S5.

Molecular structure of **(A)** the green fluorescent semiconducting dye DTTO **(B)** the red emitting ECB04 (2,5-dioxopyrrolidin-1-yl-5'-(7-(thiophen-2-yl)benzo[c][1,2,5]thiadiazol-4-yl)-[2,2'-bithiophene]-5-carboxylate. **(C)** Compound 2: [2-phenyl-6-(2-methylthiophene)-3,5-dimethyl-dithieno[3,2-b:2′,3′-d]thiophene-4,4 dioxide]. **(D)** Coumpound 3: [2-phenyl-6-(2-(2-((2-methoxyethoxy)methoxy)ethyl)thiophene)-3,5-dimethyl-dithieno[3,2-b:2′,3′-d]thiophene-4,4-dioxide]

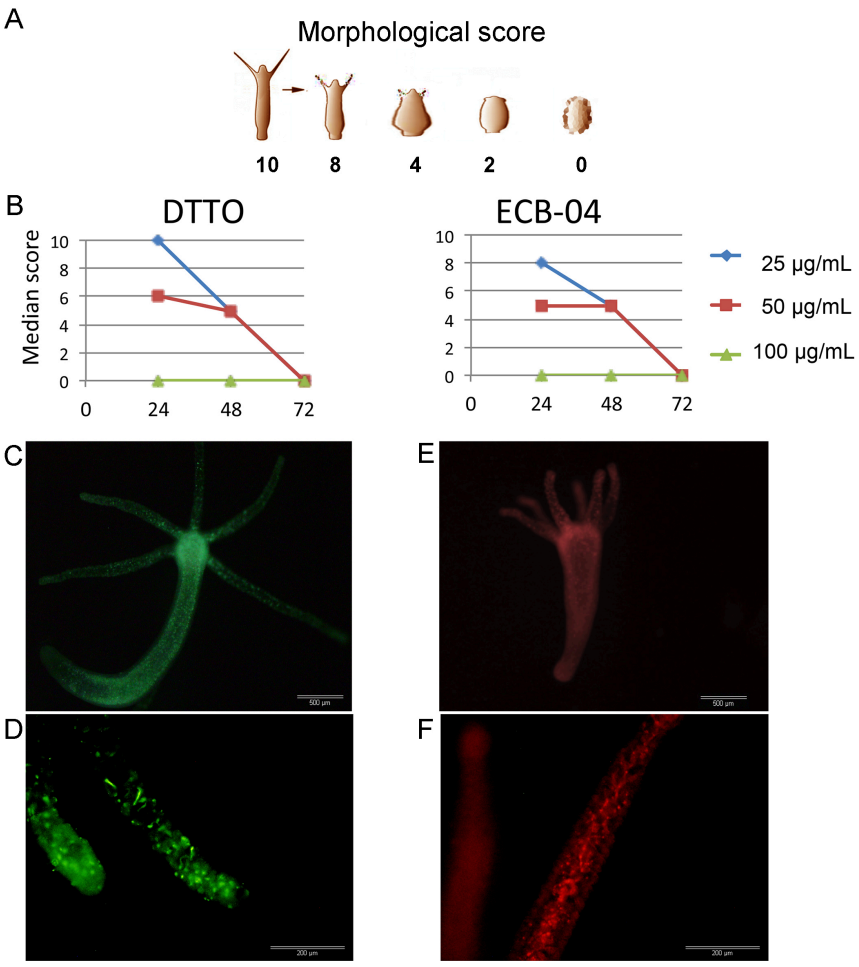

Figure S1. Toxicological evaluation of DTTO and ECB04 in *Hydra vulgaris:* chronic condition. Related to Figure 1

(A) The scheme shows progressive morphological alterations induced by the presence of a toxicant in the medium bathing living animals. The methodology is reported in the Transparent method section. **(B)** The graphs show the dose responses curve for DTTO and ECB04 (N=20). The median score value is reported as function of the incubation time. Compared to DTTO, ECB04 was slightly toxic, as indicated by the lower median score values at 24 h. **(C)** *In vivo* fluorescence imaging of a whole animal incubated with DTTO (25 µg/ml) for 24 h. **(D)** Detail of the tentacles, showing long fluorescent fibers. **(E)** *In vivo* fluorescence imaging of a whole animal incubated with ECB04 (25 µg/ml) for 24 h. The contracted shape shows the slight toxicity. **(F)** A detail of a tentacle shows the absence of biofiber production. Scale bars, 500 µm in C, E, 200 µm in D, F.

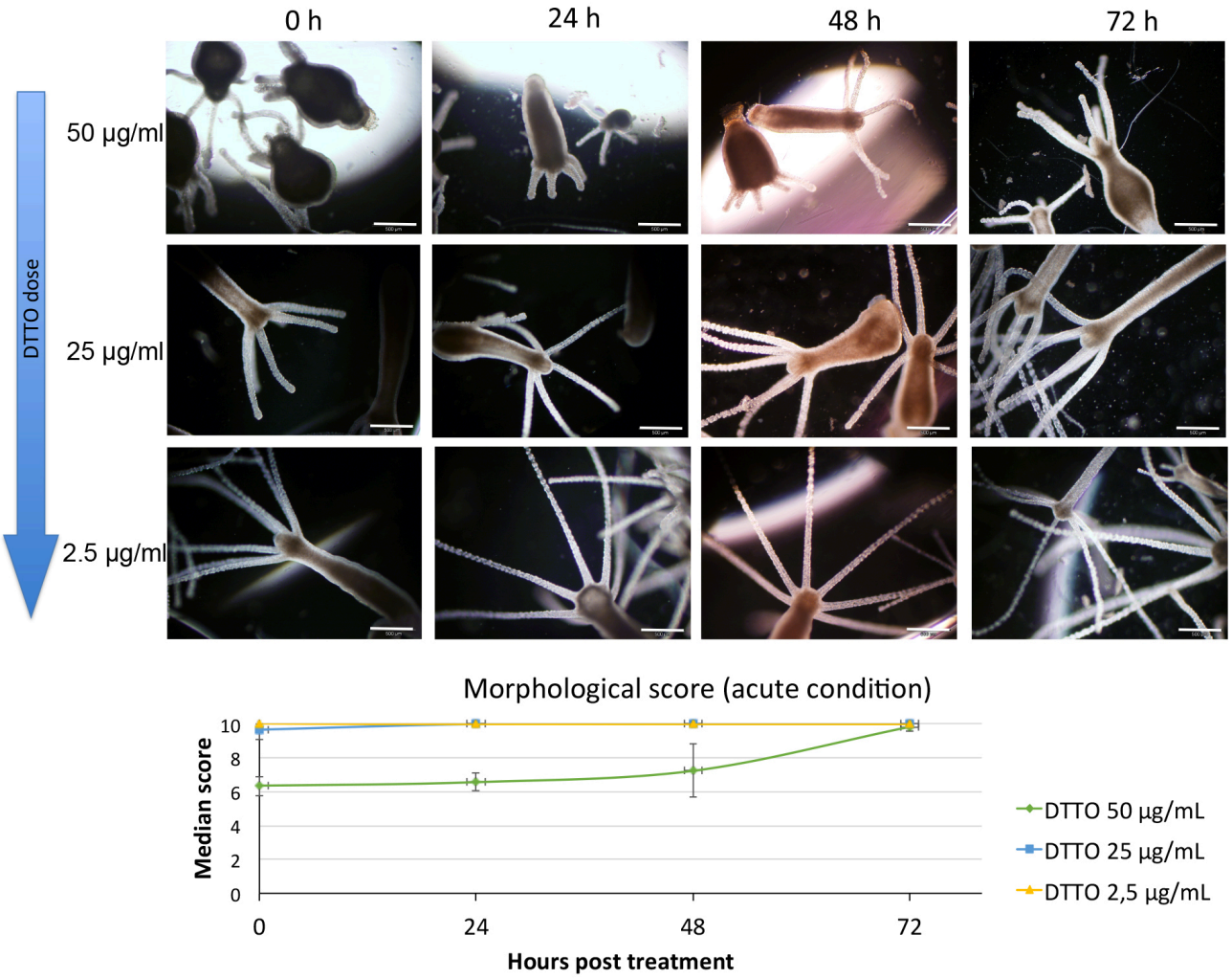

Figure S2. Toxicological evaluation of DTTO in *Hydra vulgaris:* acute condition. Related to Figure 1

Polyps were treated 5 h with DTTO at the indicated concentrations and observed at 24 h intervals post treatment. Data show biosafety of 2.5 and 25 µg/ml doses, while at t= 0 h, t= 24 h and t= 48 h post treatment animal contraction and tentacle shortening were observed, indicating a slight effect of DTTO, completely recovered at 72 h time point. Morphological scores are same as in Figure S1, ranging from 10 (healthy animal) to zero (disintegrated animal). Scale bars: 500 µm. The quantitative estimation of these toxicological traits are reported in the graph below, showing the median scores monitored on n= 60 polyps at each time point. Data represent the average of three independent experiments ± SD.

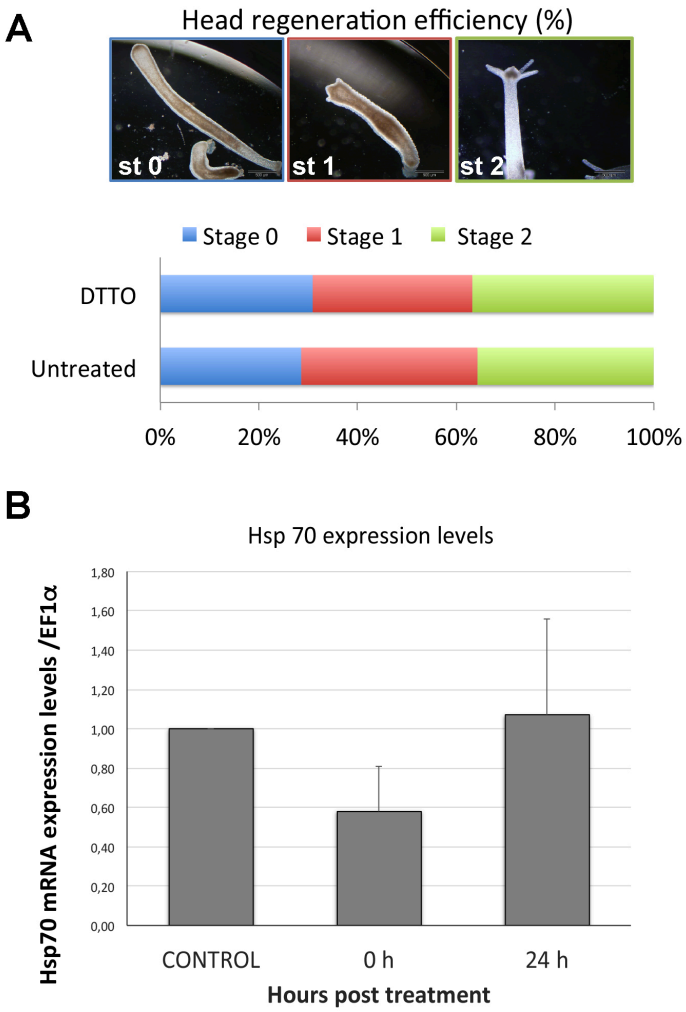

Figure S3. *In vivo* and *in vitro* toxicological evaluations of DTTO in *Hydra*. Related to Figure 1

(A) Impact of DTTO on regenerative capability of *Hydra*. The methodology is reported in the Transparent method section. Briefly, groups of 20 polyps were treated 5 h with DTTO 25 μg/mL, and after washing bisected and allowed to regenerate in fresh medium. After 24 h all polyps show wound closure and not differences between treated and untreated polyps. The graph shows the average distribution of all developmental stages, from three biological replica (n=60), at 48 h post amputation. No differences were detected between DTTO treated and untreated polyps. **(B)** Expression pattern of *Hsp70* stress responsive gene in DTTO treated polyps by qRT-PCR analysis using Elongation factor 1-alpha (Ef-1α) as reference gene. Groups of 20 *Hydra* were treated 5 h with DTTO 25 μg/mL, then washed, and after 24 h processed for qRT-PCR. Not significant differences were detected between treated and untreated animals. Statistical comparisons were performed using one sample t test.

List of primers employed for qRT-PCR

gene	accession number	Forward primer	reverse primer
Ef-1a	XP_012553476.1	ccaggagacaatgtcggttt	gcttcaatggcaggatcatt
Hsp70.1	XP_002159813	cgacgtattcagacaatcaacc	caatttgaggaacacctcttgg

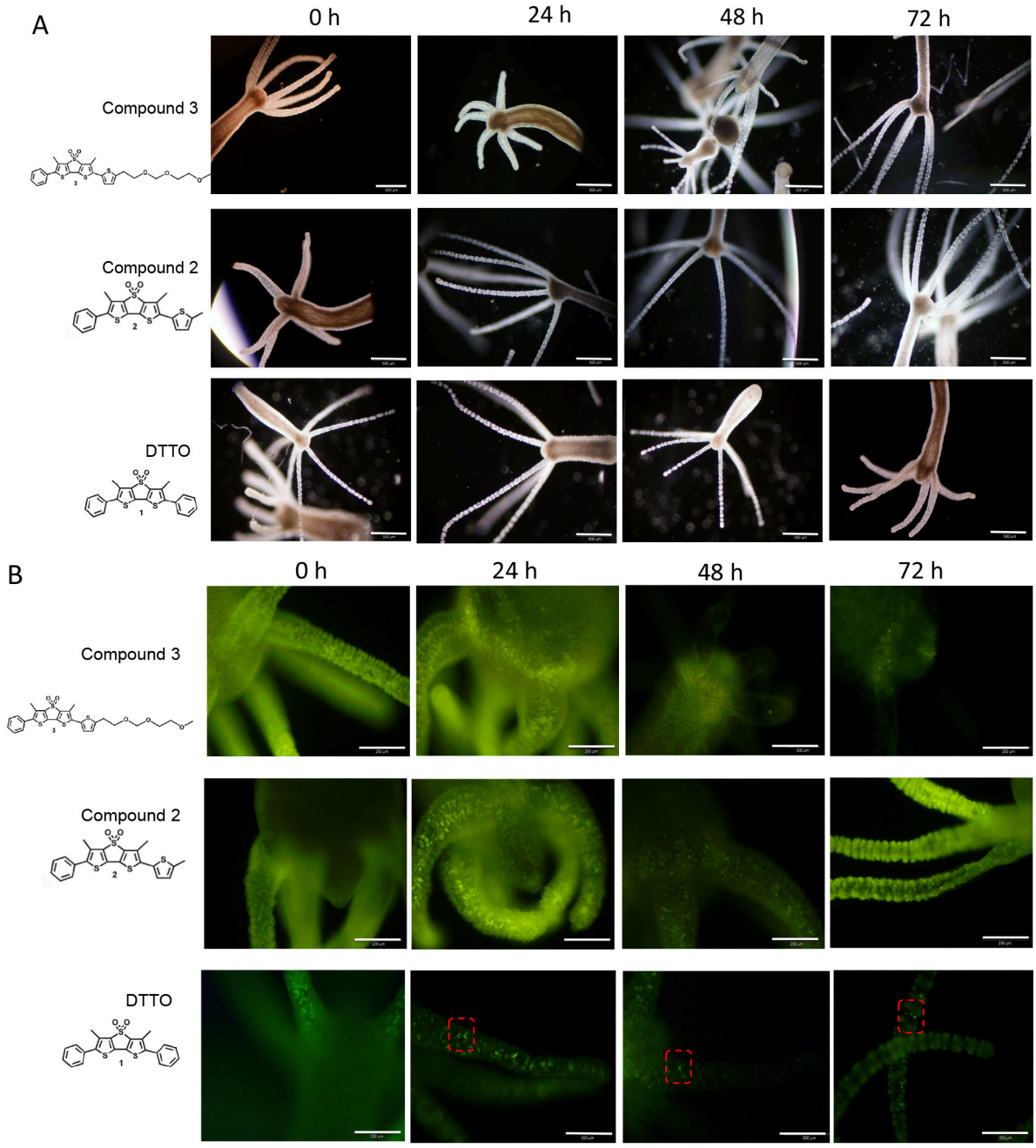

Figure S4. Biofiber production is specifically induced by DTTO and not by other oligothiophene-based fluorophores. Related to Figure 1

Group of 20 polyps were soaked for 5 h with the indicated fluorophore (time zero) and after washing monitored by fluorescence microscopy every 24 h. **(A)** Brightfield images show the absence of evident toxic effects induced by any fluorophores, as indicated by normal polyp morphology and behavior. Scale bars, 500 μm. **(B)** Fluorescence microscopy images of the same polyps showing the presence of biofibers from 24 h time point onwards only on tentacles from the DTTO treated polyps (framed by red dotted squares). Scale bars, 200 μm.

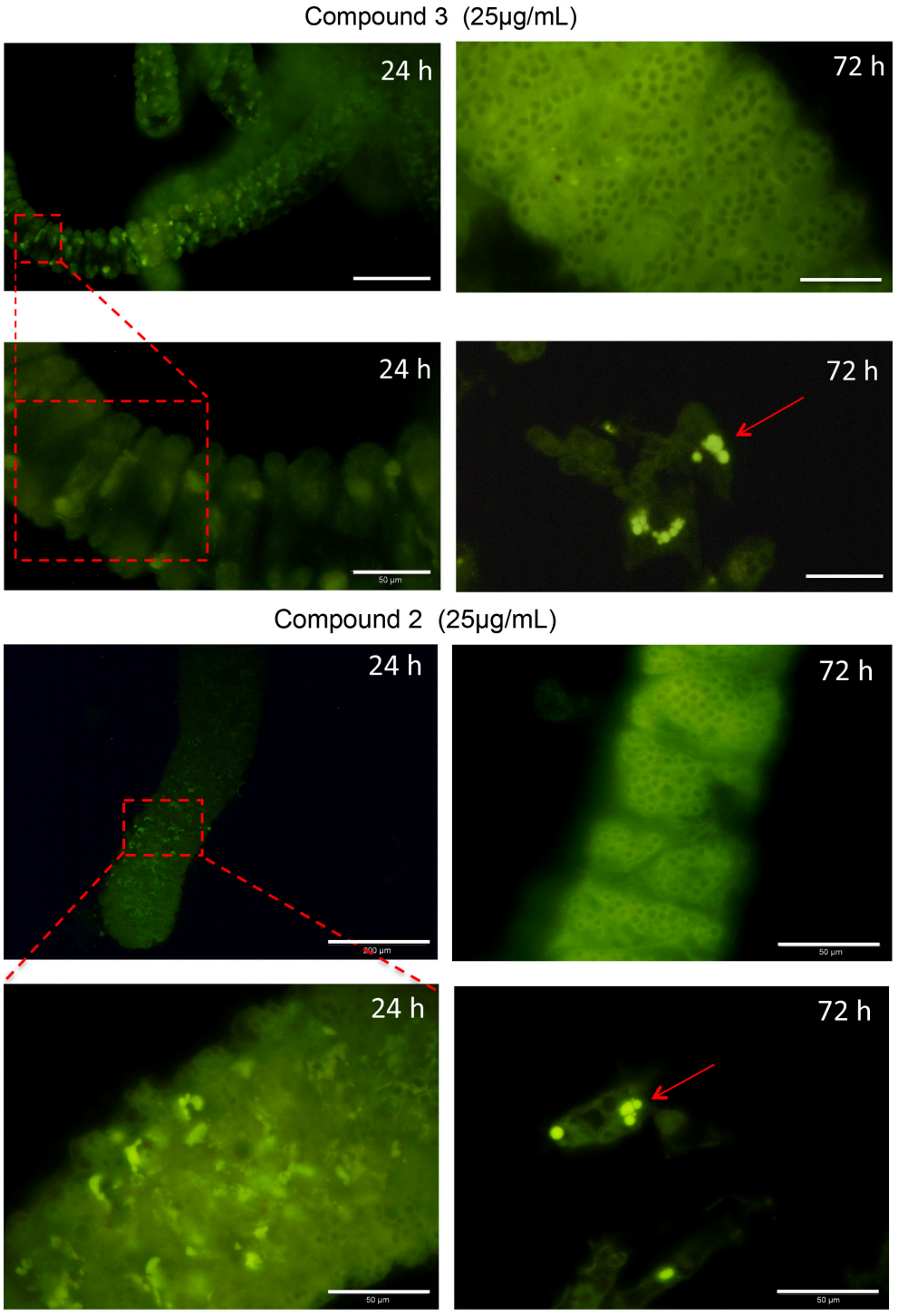

Figure S5. Effect of green emitting thiophene-based compound 2 and compound 3 on *Hydra* tissue and cells. Related to Figure 2

Treatment of polyps with compound 2 and 3 at the same doses and time as DTTO does not induce biofiber production. Animal tissues show diffuse fluorescence both at 24 h and 72 h post treatment. Detail of red square framed regions of the tentacles at 24 h time point are shown at higher magnification below. Single cells suspension prepared at 72 h by maceration of treated animals (see method section) show dye accumulation into cells (red arrows). Scale bars, 100 µm upper left images; 50 µm all others.

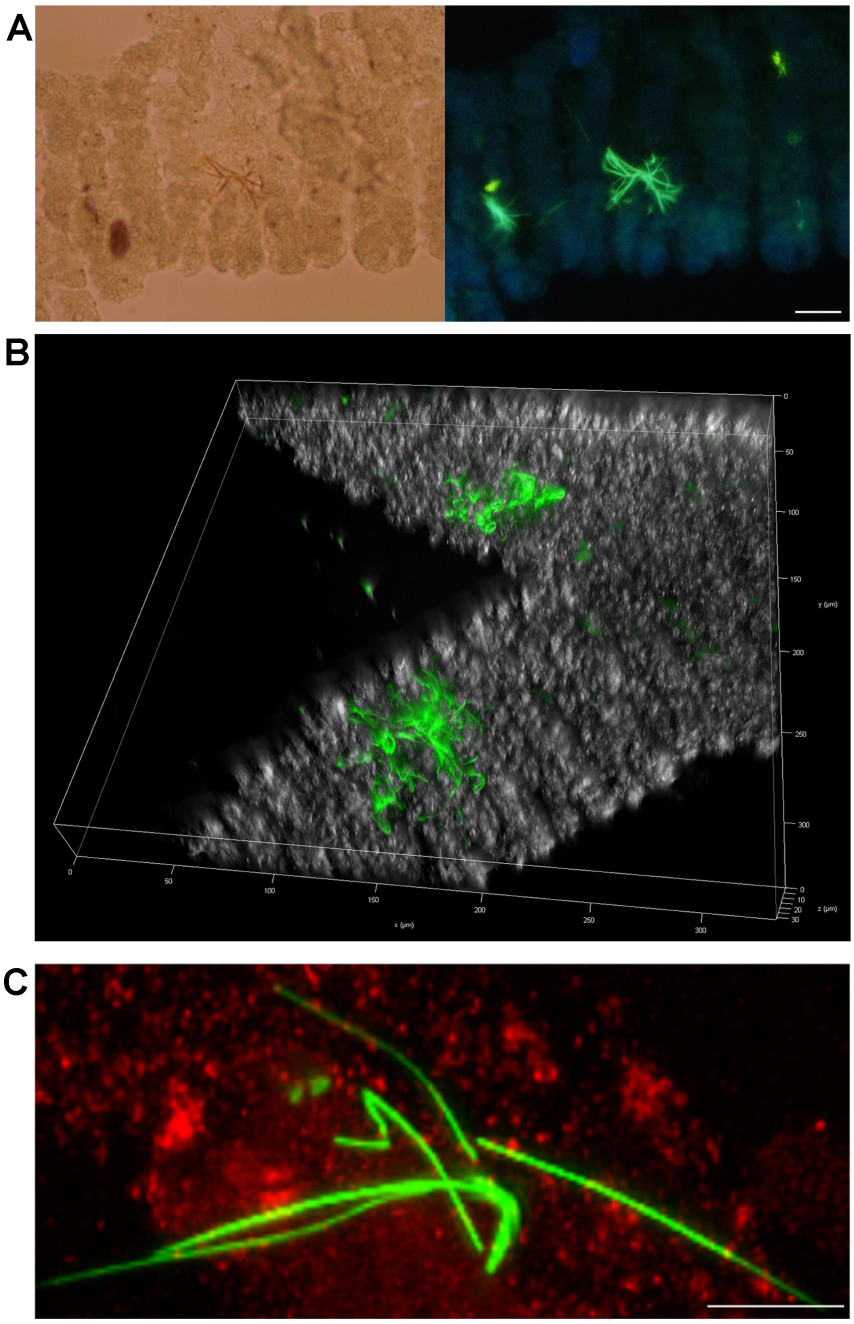

Figure S6. Imaging DTTO-based biofibers on *Hydra* tentacle. Related to Figure 1, Movie S1 and Movie S2

(A) Bright field (left) and fluorescence imaging (right) of a *Hydra* tentacle prepared by maceration from DTTO treated polyps. After 5 h incubation with 25 μg/ml DTTO, polyps were washed and left in fresh Hydra medium for 24 h. Polyps were then relaxed in 2% urethane, soaked over night into maceration solution (glycerol: acidic acid: water= 1:1:13) and fixed with 4% paraformaldehyde. Macerated cells and piece of tissues were spread on glass slide and analysed by optical microscopy. Fluorescent biofibers showing different morphologies were easily detected on the external surface of the tentacles. Scale bar, 10 μm. **(B)** Bright field and fluorescence optical merged images of *Hydra* tentacles. After 5 h incubation with 25 mg/ml DTTO, whole polyps were washed and left in fresh Hydra medium for 24 h. After relaxing in 2% urethane, polyps were fixed with 4% paraformaldehyde and mounted on microscopy slide. Image was obtained by using a Leica THUNDER Imager 3D Cell Culture microscope, 40x dry objective, NA=0.95. **(C)** Maximum Intensity Projection of the fluorescence Immunolocalization performed on *Hydra* macerates.

Immunolocalization was performed on macerates form DTTO treated Hydra using *Hydra* anti-collagen I. The methodology is reported in the Transparent method section. The image shows a green emitting fiber on the top of a cell. Cross-reaction with Hydra anti-collagen I is evident on the cell laying below the biofiber (red), but there are not clear signs of co-localization on the fiber. This may be due to the absence of Hydra collagen I inside the fibers, or to technical limits. The maceration procedure, the structural masking of the epitope due to DTTO bonding or the complexation may also prevent the cross reaction. Scale bar, 10 μm

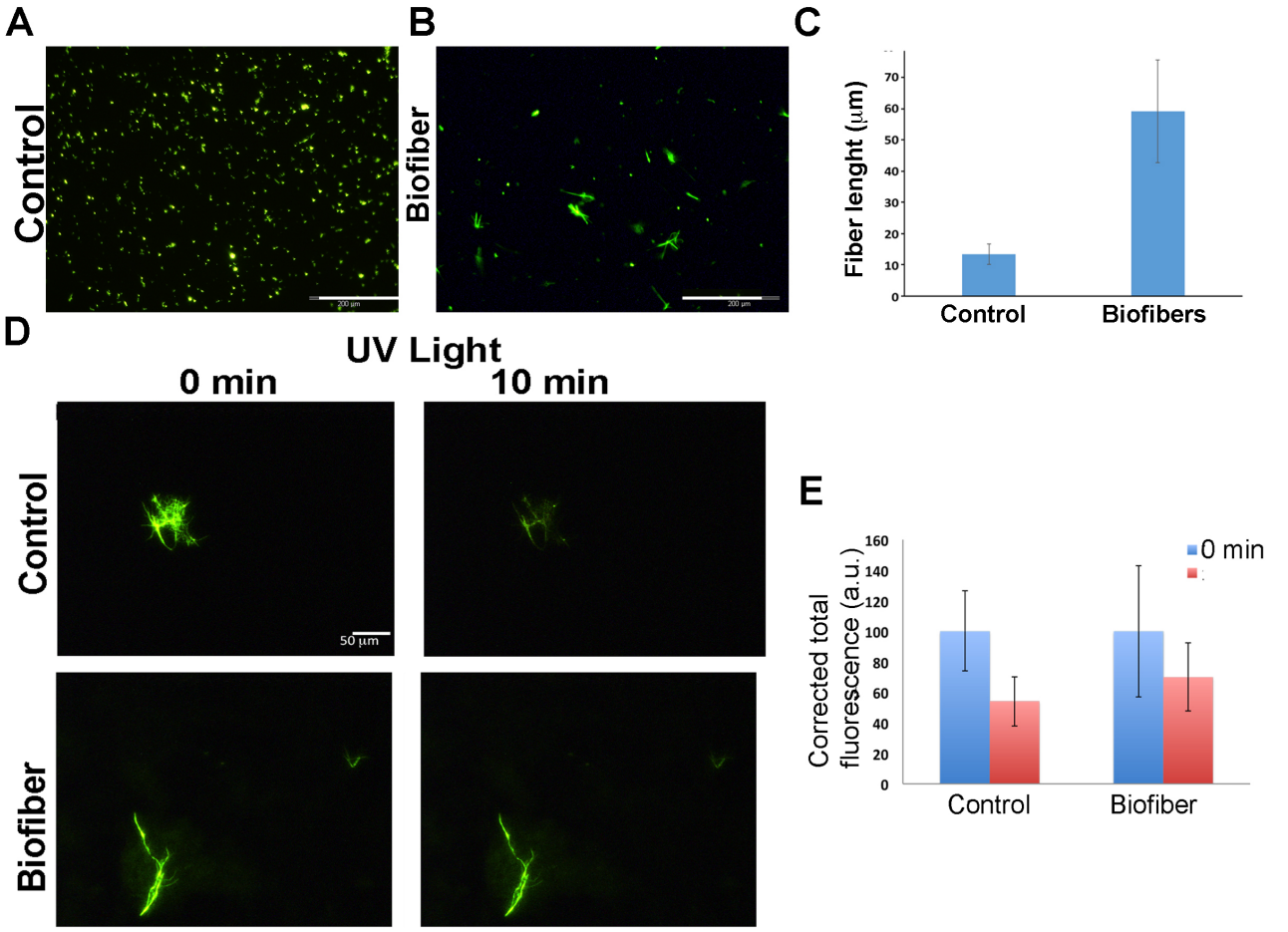

Figure S7. Structural and optical differences between DTTO aggregates and biofibers. Related to Figure 2.

(A) Spontaneous aggregates formed by DTTO in Hydra medium and **(B)** Biofibers produced by animals treated with DTTO for 5 h. **(C)** While the DTTO in solution formed small aggregates of 13.3 μm mean average length, the biofibers synthesized by the polyps present a mean length of 59.13 μm. Scale bars, 200 μm. **(D-E)** Photobehaviour of biofibers and DTTO aggregates. Aggregates formed from DTTO in Hydra medium (control) and biofibers produced by the animals were exposed to UV light for 10 min and the fluorescence intensity recorded using different regions of interest (ROI), before and after the illumination. DTTO aggregates lost 45.8 % of their initial fluorescence, while biofibers lost only 30.1%. Data represent the average from three independent experiments. Statistical comparisons were performed using one sample t test.

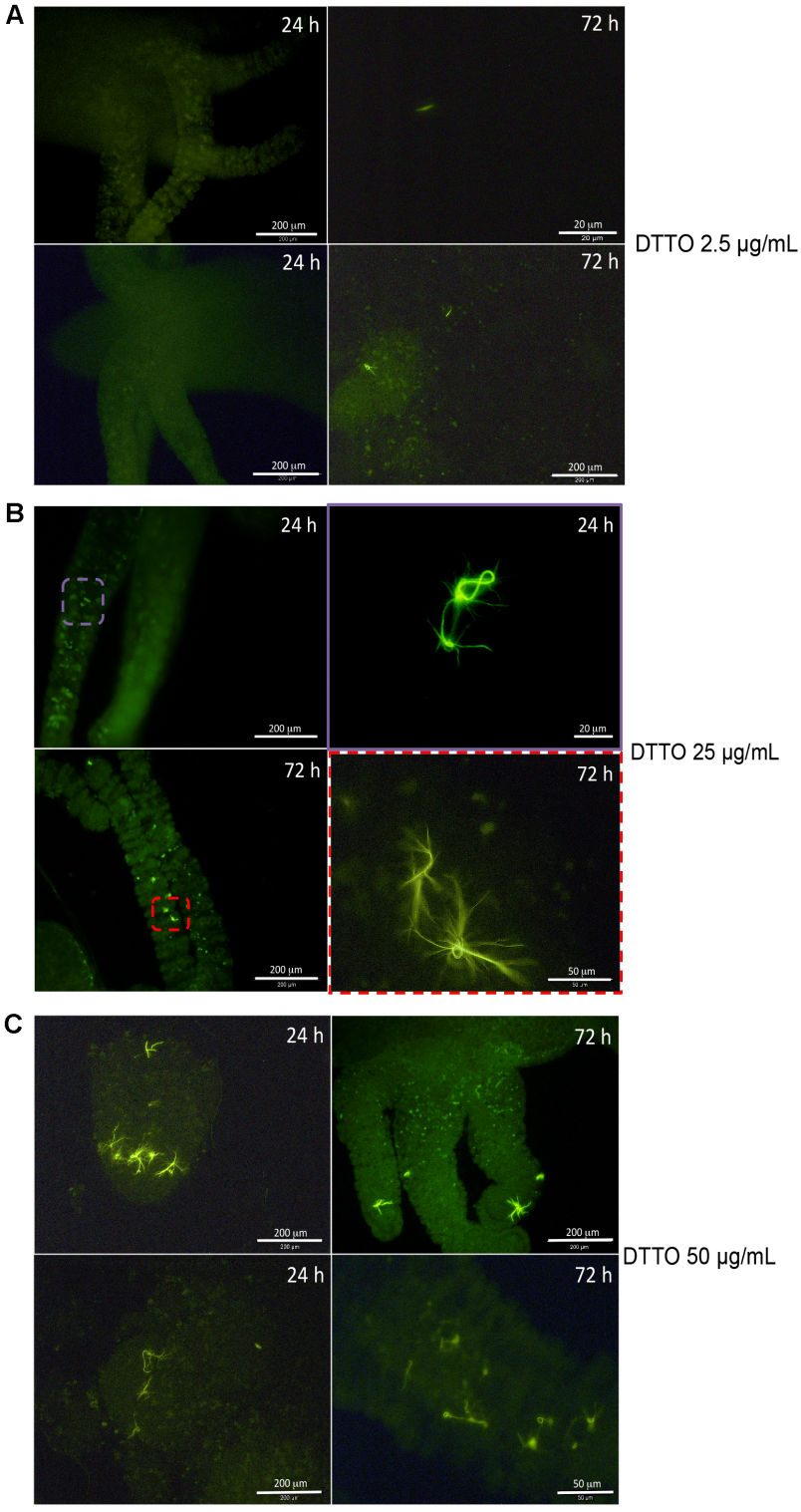

Figure S8. Biofiber efficiency of production and yield are related to the DTTO concentration and time post treatment. Related to Figure 1.

By increasing the DTTO concentration (2.5 to 50 µg/ml) and incubation period post treatment (24 to 72 hours) the average number of animals producing biofiber increases, although a high variability was found between individuals. Scale bars are indicated in each image.

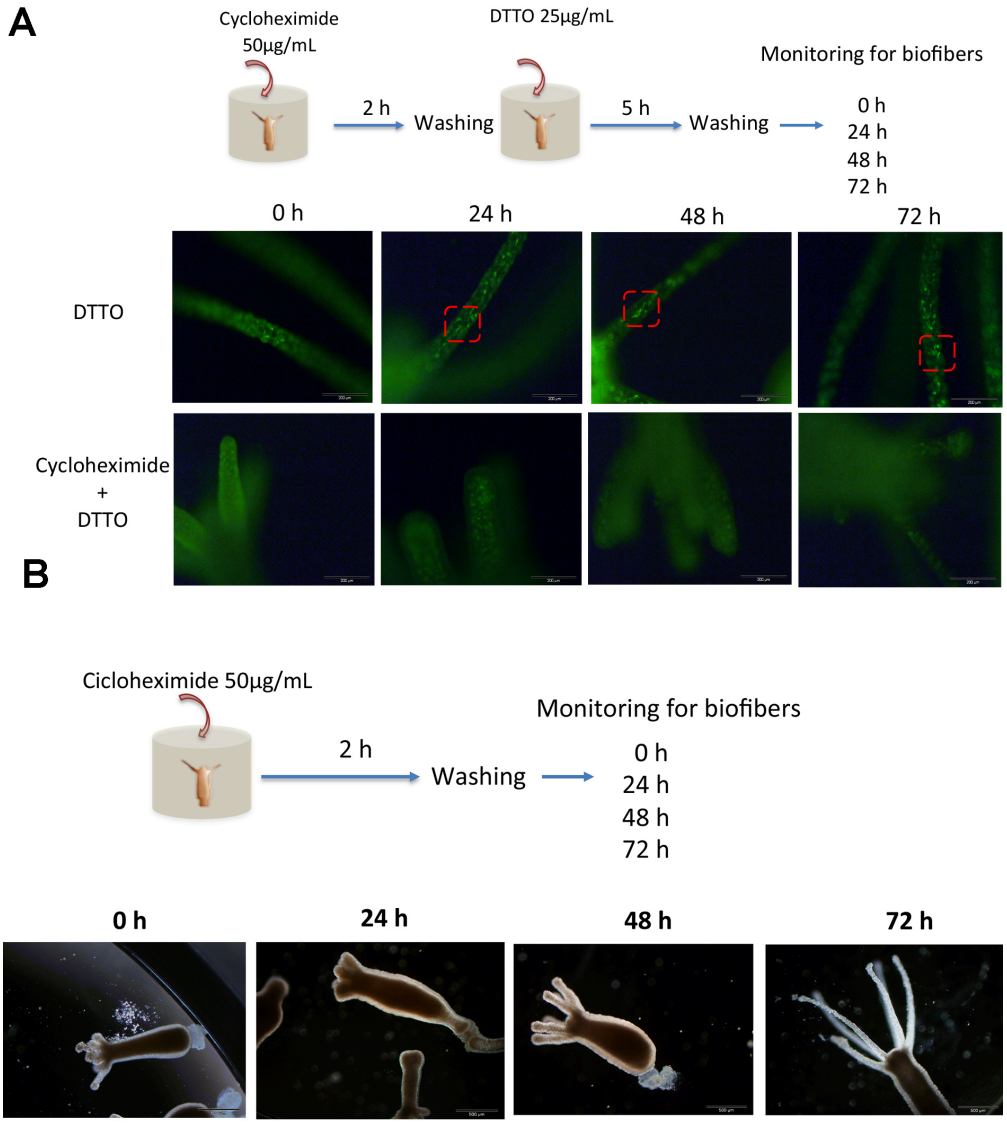

Figure S9. Biofiber formation is prevented by the protein synthesis inhibitor cycloheximide. Related to Figure 1

(A) Cycloheximide is an inhibitor of protein biosynthesis and broadly used in cell biology in terms of determining the half-life of a given protein (Kao et al., 2015, Obrig, 1971). The scheme of the experiment is shown in the upper panel. *Hydra* treated with cycloheximide (Sigma-Aldrich) only rarely produce biofibers (see Figure 1), indicating that an active process of protein synthesis is involved in biofiber production. Experiments were performed in triplicate on a total of 50 polyps. Representative polyps are shown in the images. Scale bars, 500 µm (upper images) and 200 µm (lower). **(B)** Evaluation of cycloheximide biocompatibility in *Hydra vulgaris*. Polyps were treated with cycloheximide 50 µg/mL for 2 h and polyp morphology monitored every 24 h intervals. Images show that after washing the animal morphology is rapidly recovered, indicating good biocompatibility for this drug in *Hydra*.

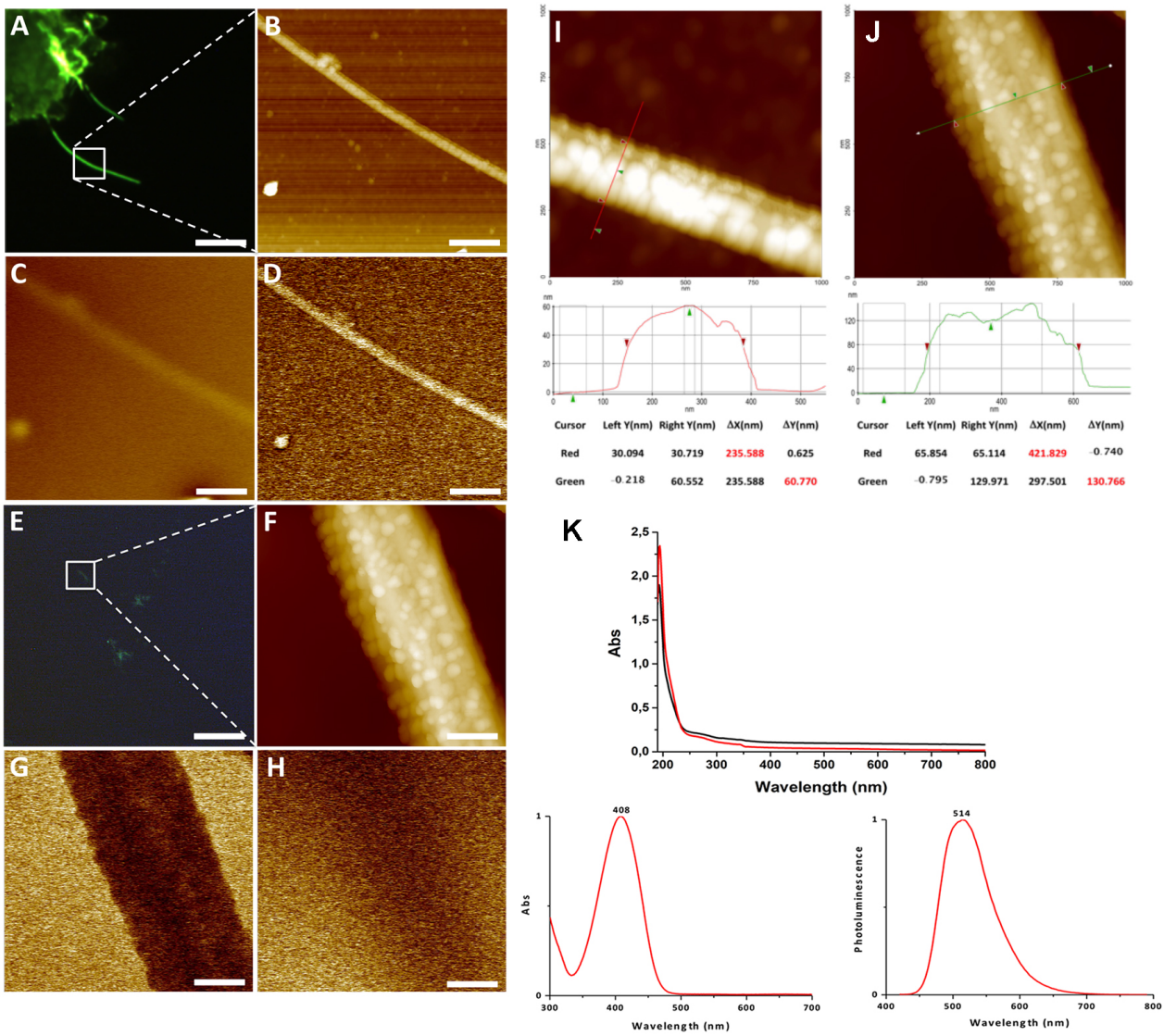

Figure S10. Electrical, morphological, and optical characterization of biofibers and DTTO aggregates. Related to Figure 3 and Figure 5

(A) Fluorescence image of a biofiber (scale bar, 50 μm). The white square shows the sub-region selected for AFM and EFM characterizations. **(B)** AFM topography (scale bar, 2 μm). EFM amplitude of the biofiber at bias voltage. **(C)** 0 V and **(D)** –10 V, respectively (scale bars, 2 μm). **(E)** Fluorescence image of a DTTO self-aggregated fragment (scale bar, 20 μm). The white square shows the sub-region selected for AFM and EFM characterizations. **(F)** AFM topography (scale bar, 200 nm). EFM amplitude of the control at bias voltage **(G)** 0 V and **(H)** –10 V, respectively (scale bars, 200 nm). **(I-K)** Characterization of biofibers and DTTO aggregates. AFM topography images on 1x1 mm^2 field, at 512x512 pixels resolution of **(I)** a biofiber produced in *Hydra* and **(J)** control, DTTO spontaneously aggregated in Hydra medium. Images are presented and analyzed on a line perpendicular to fiber direction. The height measurements on the lines are reported in the corresponding graphs and tables. **(K)** Optical characterization of macerates and DTTO aggregates. Upper panel: spectra of macerates from DTTO treated *Hydra* (black line) and untreated *Hydra* (red line). Lower: absorption and emission spectra of DTTO in methylene chloride

Time	DTTO [μg/mL]	P value	Significance
24 h	2.5 vs 25	0.0017	**
24 h	2.5 vs 50	< 0.0001	***
24 h	25 vs 50	0.0093	**
24 h	25 vs 25 (cyclohex.)	0.0018	**
72 h	2.5 vs 25	< 0.0001	***
72 h	2.5 vs 50	< 0.0001	***
72 h	25 vs 50	< 0.0001	***
72 h	25 vs 25 (cyclohex.)	< 0.0001	***
24 h vs 72 h	50	0.0037	**
24 h vs 72 h	25	0.9107	Not significant
24 h vs 72 h	2.5	0.2045	Not significant
24 h vs 72 h	25 (cyclohex.)	0.2839	Not significant

Table S1. Statistical comparisons relative to the graph of Figure 1K. Related to Figure 1

Statistical comparisons were performed using unpaired t-*test;* *, P<0.05; **, P<0.01; ***, P<0.001.

Transition	S 2p		N 1s	P 2p	C 1s	O 1s	Au 4f
Chemical state	S-C	S=O	N-C	P-O	C-C/C-N	Mixed	Au^0
Au	-	-	-	-	11.0±0.5	-	89.0±0.9
DTTO/Au	5.9±0.5	3.4±0.4	-	-	74.8±0.9	8.1±0.5	8.0±0.5
Biofibers/Au	0.13±0.05	0.12±0.05	5.1±0.5	1.7±0.2	70.6±0.9	15.7±0.7	6.2±0.5

Table S2. Atomic concentration of elements in biofibers. Related to Figure 4.

Atomic concentration of elements in Ar^+ sputtered Au, DTTO on Ar^+ sputtered Au and DTTO biofibers on Ar^+ sputtered Au. The Ar^+ sputtered Au presents no contamination from N, P, S or O. DTTO biofibers contains a c.a. 0.35% of Cl (Cl 2p signal).

Transparent methods

Animal Culture

Hydra vulgaris were asexually cultured in *Hydra* medium (1 mM $CaCl_2$, 0.1 mM $NaHCO_3$, pH=7). Animals were fed three times per week with freshly hatched *Artemia salina* nauplii at 18°C with a 12:12 h light: dark regime. Polyps from homogeneous populations without buds were selected for the experiments.

Biofiber Production

DTTO, ECB04, compound 2 and compound 3 dyes were dissolved in the minimum amount of DMSO and then diluted in Hydra solution to obtain a stock solution. Chemical concentration to use for all experiments was selected based on previous reports performed in cell cultures (Viola et al., 2013), and here tested against *Hydra* in chronic or acute condition (see below).

In a typical experiment of biofiber formation 70 *Hydra* were treated with 1mL of DTTO 25 μg/mL for 5 h in a plastic multiwell. Two control conditions were set up, *Hydra* cultured without DTTO, and DTTO in solution (25 μg/mL) without *Hydra* to characterize and differentiate fiber formation in presence or absence of animals. After incubation, all media were collected, polyps were extensively washed, maintained in 1 mL of fresh medium and continuously monitored up to 6 days post treatment by fluorescence microscopy (Nikon Eclipse Ti-E). The process of biofiber production was inhibited by the addition of Cycloheximide (Merk), a known inhibitor of the protein synthesis (Kao et al., 2015). *Hydra* polyps were pre-treated 2 h with cycloheximide (50 μg/mL) before DTTO addition, and biofiber production monitored for the following 72 h at 24 h intervals. Cycloheximide dose was selected on the bases of literature data on cell culture, where doses ranging from 50-300 μg/ml are recommended and incubation periods from 2 up to 24 h (Kao et al., 2015). We selected the lowest dose and treatment period and found biocompatibility for *Hydra* (Figure S9).

Hydra Maceration into Fixed Single Cells

Polyps were macerated to obtain single-cell suspensions and to characterize the biofibers using a solution composed by acetic acid, glycerol and H_2O in a 1:1:13 (v/v) ratio.(David, 1973) The obtained single-cell suspensions were fixed with 4% paraformaldehyde and spread on slides. After extensive washing in PBS (NaCl 137 mM, KCl 2.7 mM, Na_2HPO_4 10 mM, KH_2PO_4 1.8 mM) macerates were observed by an inverted microscope (Axiovert 100, Zeiss, JENA, GERMANY) equipped with a digital color camera (Olympus, DP70). The software system Cell F (Olympus) was used for imaging acquisition and analysis. For laser scanning confocal microscopy (LSCM) a Leica TCS SP5 microscope was used, equipped with a 100 oil immersion objective. Laser line at 488 nm for excitation was provided by an Ar laser.

In order to characterize the fibers by CD, UV-Vis, AFM and EFM, XPS and IMS the fiber content after maceration was enriched by centrifugation of the macerated suspension and water resuspension. Control samples containing DTTO in Hydra medium were also characterized using the same techniques.

UV-Visible Spectroscopy and Circular Dichroism

The samples analysed were either cell macerates containing biofibers prepared from *Hydra* (sample A) or control samples, including DTTO in methylene chloride (sample B) or DTTO in *Hydra* solution (sample C). UV-Vis and PL data were obtained using a Perkin Elmer Lambda 20 spectrometer and a Perkin Elmer LS50 spectrofluorometer, respectively. Lifetime measurements were performed with the time correlated single photon counting accessory of Fluoromax-4 using 455 nm pulsed excitation (1 MHz repetition rate). CD spectra were collected using a spectropolarimeter JASCO J-715 under ambient conditions.

Atomic Force Microscopy

Atomic and Electrostatic Force Microscopy imaging were performed with XE-100 AFM (Park Systems) and Lock-in Amplifier (SR-830) to distinguish electric force and Van der Waals force effect and obtain 3D images of fiber surfaces. Non-contact mode (NCM) was realized by oscillating metallic-silicon tips mounted on gold coated cantilevers 150 μm long with nominal resonance frequency 140-150 kHz and force constant of 7.4 N/m (PPP-NCSTAu, Park Systems). In EFM measurements an AC signal $V(t)=V_0\sin(\omega t)+V_b$ was applied to the tip using Lock-in Amplifier, where V_0 = 2 V and ω = 17 kHz and V_b was the bias voltage and was 0V, -10 V

and +10 V. Fixed cells obtained by maceration of DTTO treated animals were deposited on a gold-coated substrate in order to obtain a good conductivity of the background. As control a solution containing DTTO in Hydra medium was used. The sample preparation followed the procedure previously reported.(Cicatiello et al., 2017)·(Oliviero et al., 2017) Briefly, 5 mL aliquots of the sample/imaging buffer were directly deposited by casting onto the substrate; after 2 min, samples were gently washed with deionized water in order to remove cell and salt traces, then, dried by evaporation at room temperature under a ventilated fume hood. Fluorescent fibrils were individuated by means of fluorescence microscopy (Leica Z16 APO fluorescence microscope equipped with a Leica camera DFC320; filter sets: 450–490 nm band-pass excitation filter, a 510 nm dichromatic mirror and a 515 nm suppression filter) and then the same imaging field was analysed by AFM and EFM. The images of AFM topography and EFM amplitude have 512x512 pixel resolution and the scan frequency was typically 0.5 Hz per line. When necessary, the AFM images were processed by flattening, to remove the background slope, and to adjust the contrast and brightness.

Fourier Transform Infrared Micro-Spectroscopy (IMS)

IMS analyses were performed at beamline ID-21 at the European Synchrotron Radiation Facility (ESRF) in Grenoble, France. The beamline is equipped with a Thermo Nicolet Continuum (Thermo Scientific, Madison, WT, U.S.A.) microscope coupled to a Thermo Nicolet Nexus FTIR spectrometer (Thermo Scientific, Madison, WT, U.S.A) with a 32X objective, a motorized sample stage, and a liquid nitrogen-cooled 50 µm mercury cadmium telluride detector. Samples were mounted on BaF_2 windows (0.4 mm thick) and observed at 10x magnification using a UV illuminator to locate the fibers. After, a point outside the fiber was selected as background and a region was marked to perform mapping at 5 µm step size adding 64 scans with a resolution of 6 cm^{-1}. From this hyperspectral data set, a distribution map of amide I (1650 cm^{-1} C=O stretching vibration of the peptide bond with a minor contribution from C-N stretching vibration) was obtained after processing the spectra to second derivative (Savitzky-Golay 21 point filter and second order polynomial) and plotting the intensity at 1655 cm^{-1}. From this map 12 and 15 spectra were extracted from the fiber zone and outside, respectively. The spectra from each were averaged and plotted to observe the main changes in the region 1500-1800 cm^{-1} looking for the characteristic absorption bands of protein secondary structure amide I and amide II (Benseny-Cases et al., 2014).

X-ray Photoelectron Spectroscopy Measurements (XPS)

XPS spectra were obtained using a Phoibos 100 hemispherical energy analyser (Specs GmbH, Berlin, Germany) and Mg Ka radiation (ħω 1253.6 eV; power = 125W) in constant analyser energy (CAE) mode, with analyser pass energy of 40 eV. The overall resolution of 1.5 eV was measured and analyser was calibrated by using the Ag 3d 5/2 (368.3 eV) signals from freshly Ar^+ sputtered samples. Charging effects was corrected by calibration of Binding Energy on C 1s (285.5 eV) for all spectra. Base pressure in the analysis chamber during analysis was $2 \cdot 10^{-9}$ mbar. Data analysis and fit were performed with CasaXPS software, after Shirley background subtraction, S 2p and P 2p doublets were fitted by constant spin-orbit split ($2p_{1/2}$ -$2p_{3/2}$) of 1.18 eV and 0.86 eV respectively. More detail about instrumental configuration and data analysis can be found in a previous report (Kovtun, 2019) . Both samples were deposited on golden slides purchased from Arrandee (Germany) having an Au thickens of 250 nm and a Cr adhesive layer of 2.5 nm. Before deposition gold substrates were cleaned by 5 min acetone sonic bath and 5 min isopropanol sonic bath; slides were dried by using a N_2 gas flow. Part of organic impurities were removed by 5 min air plasma treatment (Diener, Germany). The last impurities where removed by Ar^+ ion sputtering In Ultra High Vacuum conditions. The obtained Au slides present no S, O, N, P contamination. Samples were prepared by drop-casting the solutions on freshly cleaned golden slice and blowing of pure N_2 for few minutes.

Method for Immunofluorescence on *Hydra* macerates

Hydra macerates (as described above) were spread on slides, washed thrice for 5 min with PBS, and permeabilized with PBS 0,1% tween (PBST) for 1 h. After washing with PBS, samples were blocked 2 h with 5% BSA in PBST, and *Hydra* anti-collagen I antibody (kindly provided by M. Isas, University of Chicago) was added at 1:250 dilution in PBST-BSA and incubated over night at 4°C. Following washes (5x for 5 min) the red emitting alexa-594 donkey anti-mouse secondary antibody was used to detect cross-reacting collagen I proteins on biofibers. After 2 h incubation, samples were washed with PBST and mounted on a coverslip. Samples were scanned using a CLSM, and z stacks acquired every 0.125 mm. Maximum Intensity Projection was obtained using the microscope software.

Toxicological evaluation and determination of the test dose

1) DTTO toxicity evaluation: chronic condition

Hydra is highly sensitive to organic and inorganic compounds and several approaches may be used to determinate the impact of any medium suspended compound on its physiology, i.e. morphology, reproduction rate, regeneration efficiency. As straightforward toxicological endpoint, we monitored the animal morphology in response to increasing dose of DTTO and exposure time. We used a toxicity test based on numerical scores to describe morphological alteration, adapted by our group from a previously described method used to assess the toxic effect of organic compounds on *Hydra* (Allocca et al., 2019, Ambrosone et al., 2012, Ambrosone and Tortiglione, 2013, Ambrosone et al., 2017, Karntanut and Pascoe, 2002, Wilby and Tesh, 1990). After addition of a test compound to the medium bathing living animals, the morphology is observed and a numerical score assigned to each specimen, from 10 (healthy animal) to zero (disintegrated animal). For DTTO and ECB04 dose-response curves were determined in the range of 25-100 μg/mL in chronic condition from 24 h up to 72 h.

2) DTTO toxicity evaluation: acute condition

A detailed toxicological analysis was performed by assessing several toxicological endpoints, i.e. the impact of DTTO on animal morphology, the efficiency of regeneration and the expression level of a stress responsive gene.

- Impact on morphology

Group of 20 animals were treated for a fixed period of time (5 h) to increasing concentrations (2.5 μg/ml, 25 μg/ml and 50 μg/ml) of DTTO, then washed and inspected by optical microscopy at regular intervals (Figure S2). Morphological changes were detected only at the higher dose tested, and persisted up to 48 h post treatment, recovering the normal physiology at 72 h. These data indicate that DTTO is well tolerated up to 25 μg/ml, while higher doses may slightly impact on the animal viability early after treatment.

-Impact on regeneration efficiency

Hydra possesses a unique potential to regenerate missing body parts upon amputation (Galliot et al., 2006, Bode, 2003, Holstein et al., 2003). This tightly controlled phenomenon can be impaired by the presence of toxicants into the medium (Wilby and Tesh, 1990). We have previously tested the impact of several nanocrystals on *Hydra* using this assay (Ambrosone et al., 2012, Allocca et al., 2019, Ambrosone et al., 2017) which together with the analysis of expression of stress responsive genes may provide useful clues on the toxicity of organic or inorganic compounds.

Groups of 20 *Hydra* were treated 5 h with DTTO 25 μg/mL, then washed, bisected and allowed to regenerate in fresh medium. Every 24 h developmental stages of all animals were recorded and compared to untreated animals, bisected at the same time. Results shown in Figure S3 A show not differences in the percentages of regenerating stages between the two sets of animals at 48 h post amputation (no. of polyps=60), suggesting that the DTTO treatment does not affect the regenerative capability of the polyps.

-Impact on stress responsive gene expression levels

Groups of 20 *Hydra* were treated 5 h with DTTO 25 μg/mL, then washed, and after 24 h processed for RNA extraction and quantitative real time polymerase chain reaction (qRT-PCR), using the methods previously described (Ambrosone et al., 2012), to analyze expression level of *Hsp70*. This family of proteins is considered a potent buffering system for cellular stress, either from extrinsic (physiological, viral and environmental) or intrinsic (replicative or oncogenic) stimuli (Murphy, 2013). As such, its deregulation is associated to impairment of protein homeostasis and is found in many types of cancers. The graph of

Figure S3 B shows not significant differences in the *Hsp70* mRNA expression levels between DTTO treated and untreated animals, suggesting that DTTO treatment does not cause cell stress, at least in the temporal window overlapping with biofiber production. A comprehensive molecular analysis of other genes involved in different metabolic pathways may help to identify the molecular mechanisms underlying DTTO induced biofiber production and may be object of future investigation.

Statistical Analysis

Results of the assays were expressed as mean ± standard deviation (s.d.) of three independent independent experiments. Statistical analysis was performed using the GraphPad Prism 7 software (GraphPad Software Inc., La Jolla, CA). The significance of differences was evaluated with unpaired Student's t test, with the level of significance set at probabilities of *, $P<0.05$; **, $P<0.01$; ***, $P<0.001$

SUPPLEMENTAL REFERENCES

Allocca, M., Mattera, L., Bauduin, A., Miedziak, B., Moros, M., De Trizio, L., Tino, A., Reiss, P., Ambrosone, A. & Tortiglione, C. 2019. An Integrated Multilevel Analysis Profiling Biosafety and Toxicity Induced by Indium- and Cadmium-Based Quantum Dots in Vivo. *Environ Sci Technol.* 53, 3938-3947.

Ambrosone, A., Mattera, L., Marchesano, V., Quarta, A., Susha, A. S., Tino, A., Rogach, A. L. & Tortiglione, C. 2012. Mechanisms underlying toxicity induced by CdTe quantum dots determined in an invertebrate model organism. *Biomaterials,* 33**,** 1991-2000.

Ambrosone, A., Roopin, M., Pelaz, B., Abdelmonem, A. M., Ackermann, L. M., Mattera, L., Allocca, M., Tino, A., Klapper, M., Parak, W. J., Levy, O. & Tortiglione, C. 2017. Dissecting common and divergent molecular pathways elicited by CdSe/ZnS quantum dots in freshwater and marine sentinel invertebrates. *Nanotoxicology,* 11**,** 289-303.

Ambrosone, A. & Tortiglione, C. 2013. Methodological approaches for nanotoxicology using cnidarian models. *Toxicology mechanisms and methods,* 23**,** 207-216.

Benseny-Cases, N., Klementieva, O., Cotte, M., Ferrer, I. & Cladera, J. 2014. Microspectroscopy (muFTIR) reveals co-localization of lipid oxidation and amyloid plaques in human Alzheimer disease brains. *Anal Chem,* 86**,** 12047-54.

Bode, H. R. 2003. Head regeneration in Hydra. *Dev Dyn,* 226**,** 225-36.

Cicatiello, P., Dardano, P., Pirozzi, M., Gravagnuolo, A. M., De Stefano, L. & Giardina, P. 2017. Self-assembly of two hydrophobins from marine fungi affected by interaction with surfaces. *Biotechnol Bioeng,* 114**,** 2173-2186.

David, C. N. 1973. *A quantitative method for maceration of Hydra tissue*, Wilhelm Roux Arch. EntwMech. Org.

Galliot, B., Miljkovic-Licina, M., De Rosa, R. & Chera, S. 2006. Hydra, a niche for cell and developmental plasticity. *Semin Cell Dev Biol,* 17**,** 492-502.

Holstein, T. W., Hobmayer, E. & Technau, U. 2003. Cnidarians: an evolutionarily conserved model system for regeneration? *Dev Dyn,* 226**,** 257-67.

Kao, S. H., Wang, W. L., Chen, C. Y., Chang, Y. L., Wu, Y. Y., Wang, Y. T., Wang, S. P., Nesvizhskii, A. I., Chen, Y. J., Hong, T. M. & Yang, P. C. 2015. Analysis of Protein Stability by the Cycloheximide Chase Assay. *Bio Protoc,* 5.

Karntanut, W. & Pascoe, D. 2002. The toxicity of copper, cadmium and zinc to four different Hydra (Cnidaria : Hydrozoa). *Chemosphere,* 47**,** 1059-1064.

Kovtun, A., Jones, D., Dell'elce, S., Treossi, E., Liscio, A., Palermo, V. 2019. Accurate chemical analysis of oxygenated graphene-based materials using X-ray photoelectron spectroscopy. *Carbon,* 143**,** 268-275.

Murphy, M. E. 2013. The HSP70 family and cancer. *Carcinogenesis,* 34**,** 1181-8.

Obrig, T. G., Culp, W.J., Mckeehan, W.L., Hardesty, B. 1971. The mechanism by which cycloheximide and related glutarimide antibiotics inhibit peptide synthesis on reticulocyte ribosomes. *J Biol Chem. ;246(1):174-81.,* 246**,** 174-181.

Oliviero, G., D'errico, S., Pinto, B., Nici, F., Dardano, P., Rea, I., De Stefano, L., Mayol, L., Piccialli, G. & Borbone, N. 2017. Self-Assembly of G-Rich Oligonucleotides Incorporating a 3'-3' Inversion of Polarity Site: A New Route Towards G-Wire DNA Nanostructures. *ChemistryOpen,* 6**,** 599-605.

Palama, I., Di Maria, F., Viola, I., Fabiano, E., Gigli, G., Bettini, C. & Barbarella, G. 2011. Live-Cell-Permeant Thiophene Fluorophores and Cell-Mediated Formation of Fluorescent Fibrils. *Journal of the American Chemical Society,* 133**,** 17777-17785.

Viola, I., Palama, I. E., Coluccia, A. M. L., Biasiucci, M., Dozza, B., Lucarelli, E., Di Maria, F., Barbarella, G. & Gigli, G. 2013. Physiological formation of fluorescent and conductive protein microfibers in live fibroblasts upon spontaneous uptake of biocompatible fluorophores. *Integrative Biology,* 5**,** 1057-1066.

Wilby, O. K. & Tesh, J. M. 1990. The Hydra assay as an early screen for teratogenic potential. *Toxicol In Vitro,* 4**,** 582-3.